D-4F, an apoA-1 mimetic, decreases airway hyperresponsiveness, inflammation, and oxidative stress in a murine model of asthma

S. D. Nandedkar,* D. Weihrauch,† H. Xu,* Y. Shi,* T. Feroah,§ W. Hutchins,§ D. A. Rickaby, N. Duzgunes,†† C. A. Hillery,§ K. S. Konduri,[1,§] and K. A. Pritchard, Jr.[1,2,*]**

Departments of Pediatric Surgery,* Anesthesiology,† Pediatrics,§ and Medicine,** Medical College of Wisconsin, Children's Research Institute, Zablocki Veterans Administration Medical Center, Milwaukee, WI; and Department of Microbiology,†† University of the Pacific School of Dentistry, San Francisco, CA

Abstract Asthma is characterized by oxidative stress and inflammation of the airways. Although proinflammatory lipids are involved in asthma, therapies targeting them remain lacking. Ac-DWFKAFYDKVAEKFKEAFNH$_2$ (4F) is an apolipoprotein (apo)A-I mimetic that has been shown to preferentially bind oxidized lipids and improve HDL function. The objective of the present study was to determine the effects of 4F on oxidative stress, inflammation, and airway resistance in an established murine model of asthma. We show here that ovalbumin (OVA)-sensitization increased airway hyperresponsiveness, eosinophil recruitment, and collagen deposition in lungs of C57BL/6J mice by a mechanism that could be reduced by 4F. OVA sensitization induced marked increases in transforming growth factor (TGF)β-1, fibroblast specific protein (FSP)-1, anti-T15 autoantibody staining, and modest increases in 4-hydroxynonenal (4-HNE) Michael's adducts in lungs of OVA-sensitized mice. 4F decreased TGFβ-1, FSP-1, anti-T15 autoantibody, and 4-HNE adducts in the lungs of the OVA-sensitized mice. Eosinophil peroxidase (EPO) activity in bronchial alveolar lavage fluid (BALF), peripheral eosinophil counts, total IgE, and proinflammatory HDL (p-HDL) were all increased in OVA-sensitized mice. 4F decreased BALF EPO activity, eosinophil counts, total IgE, and p-HDL in these mice. These data indicate that 4F reduces pulmonary inflammation and airway resistance in an experimental murine model of asthma by decreasing oxidative stress.—Nandedkar, S. D., D. Weihrauch, H. Xu, Y. Shi, T. Feroah, W. Hutchins, D. A. Rickaby, N. Duzgunes, C. A. Hillery, K. S. Konduri, and K. A. Pritchard, Jr. **D-4F, an apoA-1 mimetic, decreases airway hyperresponsiveness, inflammation, and oxidative stress in a murine model of asthma.** ***J. Lipid Res.*** **2011.** 52: **499–508.**

Supplementary key words apolipoprotein • airway resistance • proinflammatory lipids

Asthma is one of the most common chronic illnesses in children and adults, affecting 5–10% of the population in North America (1). Asthma accounts for the most hospitalizations and missed school and parent workdays with an estimated cost of $12 billion per year (2). It is characterized by chronic inflammation, airway hyperresponsiveness (AHR), collagen deposition, and airway remodeling, which may lead to progressive irreversible lung damage. Asthma is primarily an inflammatory disease that occurs after a triggering agent (allergen) induces the release of histamine and proinflammatory lipids from eosinophils and mast cells. Oxidative stress is believed to play important roles in the mechanisms by which asthma increases AHR and inflammation. Indeed, proinflammatory lipids, such as LTB4, have been shown to attract lymphocytes and eosinophils to the bronchial epithelium along with their associated proinflammatory cytokines and lipid mediators of inflammation to increase AHR (1, 3).

Recent reports suggest that inflammation in asthma may be influenced by lipoproteins and/or defects in lipo-

This work was supported by the National Institutes of Health grants HL061417, HL071412, HL081139, HL079937, and HL089779 and the Children's Research Foundation of the Children's Hospital of Wisconsin. Its contents are solely the responsibility of the authors and do not necessarily represent the official views of the National Institutes of Health or other granting agencies.

Manuscript received 9 November 2010 and in revised form 30 November 2010.

Published, JLR Papers in Press, December 3, 2010
DOI 10.1194/jlr.M012724

Abbreviations: AHR, airway hyperresponsiveness; apo, apolipoprotein; BALF, bronchial alveolar lavage fluid; DCF, 2',7'-dichlorofluorescin; EPO, eosinophil peroxidase; eNOS, endothelial nitric oxide synthase; 4F, Ac-DWFKAFYDKVAEKFKEAFNH$_2$; FSP, fibroblast specific protein; 4-HNE, 4-hydroxynonenal; H and E, hematoxylin and eosin; MCh, methacholine; Non-Sen, nonsensitized; OVA, ovalbumin; OVA-Sen, OVA-sensitized; ox-PC, oxidized phosphatidylcholine; p-HDL, proinflammatory HDL; POVPC, 1-palmitoyl-2-oxovaleroyl-sn-glycero-3-phosphorylcholine; TGF, transforming growth factor.

[1] K.S.K. and K.A.P. contributed equally to this work as senior authors.

[2] To whom correspondence should be addressed.
e-mail: kpritch@mcw.edu

The online version of this article (available at http://www.jlr.org) contains supplementary data in the form of one figure and supplemental references.

protein metabolism. In 2005, ABCA1, representing the first step in reverse cholesterol transport, was reported to be essential for maintaining normal lipid composition, architecture, and airway physiology of the lung (4). In 2009, genetic deletion of endothelial lipase was shown to increase HDL nearly 2-fold, which was credited with decreasing AHR and pulmonary inflammation in ovalbumin (OVA)-sensitized mice (5). In 2010, we reported that genetic deletion of apolipoprotein (apo)A-I specifically increased pulmonary inflammation and AHR without impairing peripheral vascular function (6). Taken together, these reports suggest that perturbations in usual lipoprotein metabolism may influence experimental asthma. Further, these reports indicate that apoA-I and HDL play important and likely specific anti-inflammatory roles in protecting the lung.

Ample evidence exists to link oxidative stress to airway disease (7, 8). In 2003, it was suggested that because oxidized LDL increases recruitment of granulocytes, it may act as an important mediator of bronchial inflammation (9). Although no relationship was reported to exist between asthma and concentrations of LDL or HDL, patients with asthma typically have higher concentrations of oxidized LDL and lower concentrations of paraoxonase-1, a deficiency that is well recognized for increasing HDL oxidation and impairing HDL function (10). More recently, clinical studies revealed that asthma decreases glutathione and increases glutathione disulfide in the fluid lining airway epithelium and that this shift in glutathione balance worsens in individuals with airway obstruction (11). These reports indicate that lungs of asthmatic subjects experience greater levels of oxidative stress than the lungs in nonasthmatic subjects and that this increase in oxidative stress in the lung may promote oxidation of LDL and HDL. In atherosclerosis, such shifts in oxidative stress are believed to play important roles in accelerating lesion formation. Interestingly, chronic states of oxidative stress and inflammation are credited with converting anti-inflammatory HDL into proinflammatory (p)-HDL, which may even participate in the inflammatory processes (12, 13). Whether or not the oxidative stress and inflammation associated with asthma increase p-HDL remains unknown.

4F (Ac-DWFKAFYDKVAEKFKEAFNH$_2$) is an amphipathic, α helical peptide that functions as an apoA-I mimetic (14, 15). Previously, we showed that 4F improved endothelium-dependent vasodilatation in three diverse murine models of vascular disease: hypercholesterolemia, sickle cell disease (16), and systemic sclerosis (17). In tight-skin mice, a murine model of systemic sclerosis, intraperitoneal 4F treatments also reduced the levels of p-HDL (17). As 4F decreases inflammation and improves vascular function in such a diverse array of murine models of vascular disease, we wondered if 4F was capable of inhibiting pulmonary inflammation and AHR in experimental asthma. To test this hypothesis, C57BL/6J mice were sensitized to OVA to induce experimental asthma (18) and then treated intranasally with 4F. Our findings indicate that 4F is a potent inhibitor of AHR, pulmonary inflammation, and collagen deposition in lungs of mice with experimental asthma. Accordingly, 4F may be useful for limiting the effects of allergen-induced airway disease in asthma.

METHODS

Animals

All protocols using mice were approved by the Institutional Animal Care and Use Committee (IACUC) of the Medical College of Wisconsin and Zablocki Veterans Administration Medical Center.

4F

4F was synthesized using all D-amino acids as previously described (19, 20). Scrambled D-4F was synthesized with the same D-amino acids as D-4F but in a sequence (Ac-DWFAKDYFKKAFVEEFAK-NH$_2$) that does not promote formation of an α-helix.

Ovalbumin sensitization

On day 0, heat coagulated OVA (Grade II, Sigma Chemical Co., St Louis, MO,) was inserted subcutaneously on the dorsal aspect of the cervical region of 6-8 wk old male C57BL/6J mice. On days 14–24, the mice were exposed to 30 min aerosolization of an OVA (6%) solution in PBS on alternate days for a period of 10 days as described (18). Thereafter, mice were exposed to aerosolized OVA (6%) twice a week until euthanasia.

4F treatments

Intranasal 4F treatments were initiated on day 25. The experimental test groups were nonsensitized (Non-Sen) mice treated with PBS (30 μL) or 4F in PBS (20 μg in 30 μL) and OVA-sensitized (OVA-Sen) mice treated with PBS or 4F (20 μg in 30 μl of PBS) once a day for 4 weeks for initial histology and AHR studies. At the time of euthanasia, samples were collected from a separate set of mice for eosinophil peroxidase (EPO) in bronchial alveolar lavage fluid (BALF), lung histology, peripheral blood eosinophils, total IgE, and p-HDL levels as we described before (19, 21). Scrambled D-4F (20 μg in 30 μL PBS) was used as a peptide control in place of 4F in PBS in OVA-Sen mice compared with OVA-Sen mice treated with PBS alone.

Airway resistance

AHR measurements in response to methacholine (MCh) were performed on Non-Sen PBS controls (±4F) and OVA-Sen (±4F) mice. As an antigen challenge and to demonstrate sensitization, mice were exposed to aerosolized OVA (6%) 24 h before AHR studies.

To assess AHR, all mice were anesthetized by an intraperitoneal injection of pentobarbital sodium (= [wt (kg) × 90 mg/kg] / 5 mg/ml). Anesthetized mice were placed on a 37°C heating pad to maintain core body temperature. After confirming anesthesia by absence of pain reflex (paw pinch), mice were tracheostomized and intubated with a 1/2 inch long thin walled metal tube (0.05 in outside diameter, 0.042 in inside diameter). Mice were then connected to a computer-controlled small animal ventilator (flexiVent, SCIREQ, Montreal, PQ, Canada) and ventilated at a tidal volume of 9 ml/kg at a frequency of 150 breaths/min (default ventilation for mice) (22–25). A positive end-expiratory pressure of 3 cmH_2O was applied to the breathing circuit by submerging the outlet of the expiratory line 3 cm below the water surface in an Erlenmeyer flask.

After the mice were instrumented, they were paralyzed with an intraperitoneal injection of pancuronium bromide (0.04 μg/kg)

to eliminate the possibility of involuntary smooth muscle cell contraction during airway studies. The position of the mice was carefully adjusted and assessed with standardized pulmonary tests until a minimal airway resistance was verified. AHR was assessed using forced oscillation techniques and Prime-2 perturbations. Briefly, a Prime-2 perturbation is a forced 2 s pause in ventilation. The testing protocol for measuring AHR started with two pressure limited total lung capacity maneuvers with an intervening period of 30 s.

AHR was then assessed by administering a series of progressively increasing concentrations of MCh to induce successive increases in bronchoconstriction (26, 27). Positive end-expiratory pressure was set at 3 cmH_2O. The MCh challenge was performed at six different concentrations (1.25, 3.125, 6.25, 12.5, 18.0, 25.0 mg/ml dissolved in physiological buffered saline), which was aerosolized and vented into the anesthetized mouse using an ultrasonic nebulizer (Aeroneb, SCIREQ) connected in-line through the inspiratory arm of the flexiVent. The aerosolized MCh was administered for a total of 20 breaths at a tidal volume of ~0.4 ml at a rate of 30 breaths/min. Immediately following MCh delivery, the nebulizer was quickly removed from the inspiratory arm of the flexiVent and default ventilation reinstated. Then for the next 3 min, a Prime-2 perturbation was repeatedly applied every 20 s.

The pressure and flow data obtained during the application of each Prime-2 perturbation have been described before (22, 24, 28). Briefly, these data were used to calculate a complex input impedance of the respiratory system (Zrs). Zrs was then fit to a model consisting of a single airway serving a constant-phase viscoelastic tissue unit (29). Data analysis yields calculations for R_N ($cmH_2O \bullet s \bullet ml^{-1}$), which is Newtonian resistance composed mostly of flow resistance in conduit airways; G ($cmH_2O \bullet ml^{-1}$), which reflects viscous dissipation of energy in the respiratory tissues (tissue dampening/resistance); and, H ($cmH_2O \bullet ml^{-1}$), which reflects elastic energy storage in the tissues (tissue elastance/stiffness). The peak values for R_N, G, and H were averaged for each mouse. Raw values for R_N, G, and H were expressed as the mean ± SEM for each experimental test group.

Histopathology

The standard protocol for fixing the lungs was to inflate the lung with 0.5 ml PBS-Zn-formalin prior to removal. The tissues were embedded in paraffin, sections cut (5 μm), and stained either with hematoxylin and eosin (H and E) to enhance cytoplasmic and nuclear structures or with McLetchie's trichrome to visualize collagen. Images were captured on a Zeiss Imager.Z1 microscope using 40×/0.95 aperture objective and Axiocam HRc camera and Axiovision Software (version 4.6) (all from Carl Zeiss, Heidelberg, Germany).

Immunofluorescence studies: effects of OVA sensitization and 4F treatments on activation of TGFβ-1, FSP-1 expression, T15 autoantibodies, and 4-HNE Michael's adducts in the lung

Immunofluorescence was performed on 5 μm sections of the fixed lungs. Two sections were mounted on each slide. Sections were deparaffinized with xylene (three changes) and dehydrated in a descending alcohol row. The sections were incubated separately with rabbit polyclonal antibodies against transforming growth factor (TGF)β-1 and fibroblast specific protein (FSP)-1 (1:50 for TGFβ-1 and 1:100 for FSP-1; Santa Cruz Biotechnology, Santa Cruz, CA). T15-type autoantibodies against oxidized phosphatidylcholine [ox-PC, specifically, 1-palmitoyl-2-oxovaleroyl-sn-glycero-3-phosphorylcholine (POVPC)] were detected with a murine anti-T15 idotype antibody (30, 31); and a rabbit anti-4-hydroxynonenal (4-HNE) Michaels's adduct antibody (Calbiochem-EMD, LaJolla, CA) incubated for 30 min at 37°C. An Alexa Fluoro 488 goat anti-rabbit antibody (catalog no. A11008, Invitrogen-Molecular Probes, Eugene, OR) was used to detect anti-TGFβ-1, anti-FSP-1, and anti-4-HNE Michael's adduct antibodies. The anti-T15 antibody was isolated from peritoneal fluid from mice that were injected with a hybridoma cell line that was kindly provided by Dr. John Kearney (University of Alabama at Birmingham, Birmingham, AL). The monoclonal anti-T15-idiotypic antibody is called AB1-2 and is a mouse IgG1, which is absolutely specific for both the canonical T15 $V_H + V_L$ regions (32). The slides were washed with PBS three times and then incubated with Alexa Fluoro 488 goat anti-mouse IgG_{H+L} (catalog no. A11001; Invitrogen-Molecular Probes) for 30 min at 37°C. Negative control slides were sections stained with Alexa Fluoro 488 goat anti-mouse IgG_{H+L} or Alexa Fluoro 488 goat anti-rabbit polyclonal antibodies alone (i.e., no primary antibody). Nuclei were counterstained for 3 min at room temperature with TO-PRO-3 iodide (Ex/Em = 642 nm/661 nm, respectively; catalog no. T3605; Invitrogen-Molecular Probes). The slides were washed and mounted, and images captured on a krypton argon laser Nikon Eclipse TE2000U confocal microscope (Melville, NY) using 10×/0.17 aperture objective with the total magnification of 100 (Ex/Em = 488 nm/580 nm for FITC and 633 nm/661 nm for TO-PRO-3) and IBM EXC1 software (Armonk, NY). NIH Image J software was used to calculate fluorescent intensity relative to TO-PRO3 as previously described (17, 33).

EPO activity in BALF and peripheral blood eosinophils

At the time of euthanasia, the trachea was cannulated with a ball-tipped 24 gauge needle, lungs lavaged with PBS (0.8 ml), and samples frozen at −70°C. The samples were later thawed and assayed for EPO activity as previously described (18). Briefly, substrate solution consisting of 0.1 M Na Citrate, O-phenylenediamine, and H_2O_2 (3%), at pH 4.5, was mixed with BALF supernatants 1:1. The reaction mixture was incubated at 37°C and the reaction was stopped by adding H_2SO_4 (4N). Horseradish peroxidase was used as a standard. EPO activity (Units) was quantified by measuring absorbance at 490 nm.

Peripheral blood smears were stained with Wright-Giemsa solution. Percent blood eosinophils were calculated from the number of eosinophils per 100 white blood cells counted under a high power field (100×).

Total IgE

Total IgE was quantified by ELISA. Briefly, 96-well flat-bottom polystyrene microplates (Fisher Scientific, Hampton, NH) were coated with anti-mouse IgE (2 μg/ml, 100 μL/well, 4 h at room temperature, then 12 h at 4°C; BD Biosciences Pharmingen, San Diego, CA). After washing with PBS-Tween, the plates were blocked with 1% BSA (Sigma-Aldrich, St Louis, MO) for 1 h and the wells washed again. Serially diluted standards and test samples were then added to the plate and incubated for 12 h at 4°C. Following another set of washes, biotinylated anti-mouse IgE was added to the well (room temperature, 1 h; BD Biosciences Pharmingen). Excess biotinylated antibody was removed by washing and the wells were incubated with streptavidin peroxidase (1 h, room temperature; Sigma-Aldrich). After washing the plate with PBS (200 μL, 3×), the reaction was started by adding 100 μL/well of O-phenylenediamine-substrate [30 mg OPD in 50 ml sodium citrate, pH 4.0, with 0.25 ml of H_2O_2 (3%)]. The reaction was stopped by addition of H_2SO_4 (2N, 50 μL/well). Absorbance was read at 490 nm using a Biotek EL312e plate reader (Winooski, VT).

Total cholesterol and p-HDL

Total cholesterol was quantified using a cholesterol esterase/oxidase kit from Wako Chemical, Inc. (Richmond, VA). HDL was isolated from whole plasma with a solution of dextran-sulfate-$MgCl_2$ (10 g/L, 0.5 M; Berkeley HeartLab Inc, Alameda, CA), which precipitates apoB containing lipoproteins. HDL cholesterol was quantified using an HDL Cholesterol E kit from Wako Diagnostics. Relative rates of 2',7'-dichlorofluorescin (DCF) have been shown to provide a sensitive index of the levels of seeding molecules of lipid hydroperoxides in isolated HDL (34). An aliquot of 1 μg of HDL cholesterol from the supernatants of the dextran sulfate precipitate was incubated with $CuCl_2$ (5 μM, final concentration) for 1 h in a 384-well microtiter plate from MJ Research, Inc. (Waltham, MA). After preincubation, 10 μl of DCF (0.2 mg/ml) was added to the HDL-Cu^{2+} mixture in a total volume of 30 μl. DCF fluorescence (Ex 485 nm; Em 530 nm) was measured at 30 min intervals over the next 2 h on an LJL Biosystem Analyst™ HT (Molecular Devices Corp., Sunnyvale, CA). Rates of DCF fluorescence (units of fluorescence/min) were calculated and expressed as mean ± SEM.

Statistical analysis

Data are presented as the mean ± SEM. Statistical analysis was either one-way ANOVA with an appropriate post hoc test for determining levels of significance among means of different groups or two-way ANOVA with an appropriate post hoc test to determine significance between response curves of the different groups (* $P < 0.05$; ** $P < 0.025$; *** $P < 0.01$).

RESULTS

Airway hyperresponsiveness

OVA-sensitization markedly increased airway resistance in response to MCh challenge. Intranasal 4F treatments of Non-Sen mice decreased airway resistance with respect to R_N, an index of Newtonian resistance, in response to a MCh compared with normal mice treated with just PBS. In addition, 4F treatments of OVA-Sen mice reduced airway resistance for R_N at the highest concentration of MCh compared with the levels for OVA-Sen mice treated with PBS (**Fig. 1A**). OVA-Sen mice had increased airway resistance with respect to G, a measure of tissue dampening (Fig. 1B). The increase in G was significant with respect to interactions between groups as well as with respect to individual MCh concentrations. Further, 4F treatments reduced G below the levels observed in normal mice treated with PBS (Fig. 1B). OVA-sensitization markedly increased H, a measure of tissue elastance (Fig. 1C). The increase in H was significant with respect to both the dose of MCh as well as between test groups (Fig. 1C). Throughout the study, intranasal PBS treatments had little effect on AHR.

Histopathology

OVA-sensitization increased eosinophil and polymorphonuclear neutrophil infiltration in the lungs of the mice compared with NonSen mice (**Fig. 2A**) In contrast, 4F treatments (PBS+D-4F) markedly reduced infiltration of inflammatory cells (Fig. 2A). OVA-Sen mice had increased perialveolar and perivascular collagen deposition whereas 4F treatments (PBS+D-4F) reduced collagen deposition to

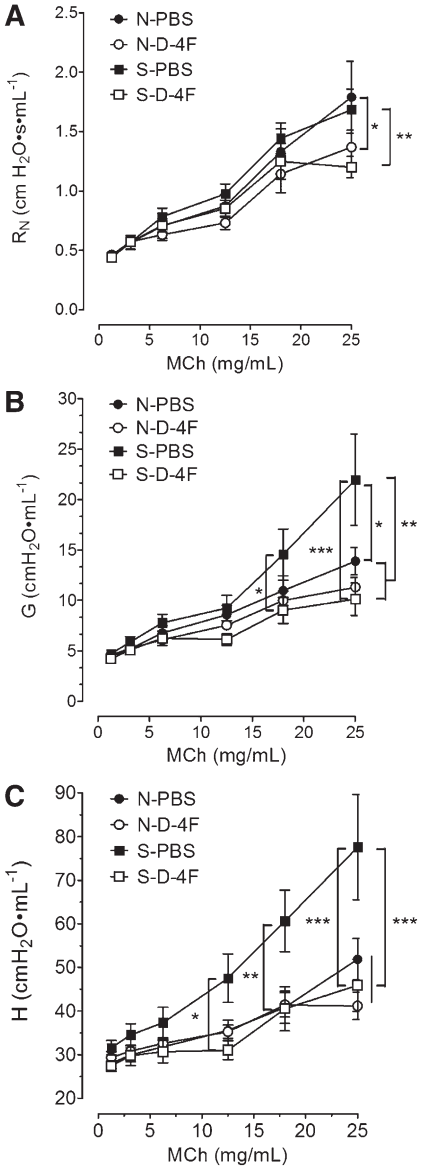

Fig. 1. Effects of ovalbumin and D-4F on airway hyperresponsiveness to methacholine (MCh) challenge. Line graphs showing that OVA sensitization increases airway resistance to MCh challenge with respect to large airways R_N, Newtonian resistance (A), tissue damping, G, (B), and tissue elastance, H, (C) and that 4F treatments reduce these measures to baseline. Line graphs for PBS-treated mice suggest that the PBS in which the D-4F was dissolved did not contribute to airway hyperresponsiveness. (N-PBS, Non-Sen PBS-treated, n = 11; N-D-4F, Non-Sen D-4F in PBS treated, n = 11; S-PBS, OVA-Sen PBS-treated, n = 10; S-D-4F, OVA-Sen D-4F-treated, n = 10).

levels that appeared similar to those in Non-Sen PBS control mice (Fig. 2B). These histology data indicate that PBS treatments alone had little effect on pulmonary inflammation or collagen deposition. To control for the possibility that 4F reduced inflammation and collagen deposition by its antioxidant properties associated with composition (35) rather than its unique biophysical structure, OVA-Sen mice were also treated intranasally with scrambled D-4F. The images in **Fig. 3** show that scrambled D-4F had no effect on recruitment of inflammatory cells or collagen deposition in OVA-Sen mice.

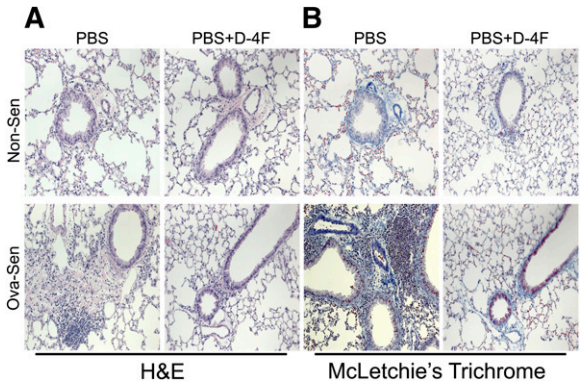

Fig. 2. Histology: effects of OVA sensitization and D-4F on pulmonary inflammation and collagen deposition. A: Representative H and E images of sections of lungs from control, nonsensitized C57BL/6J mice (upper left) and OVA-sensitized C57BL/6J mice (lower left). Treatment of OVA-Sen mice with 4F reduced infiltration of inflammatory cells into the lung parenchyma (upper right panel vs. lower right panel). B: Representative McLetchie's trichrome images of sections of lungs isolated from control, nonsensitized C57BL/6J mice (upper right) and OVA-sensitized C57BL/6J mice (lower right). 4F treatments decreased collagen deposition in the OVA-Sen mice (upper right panel vs. lower right panel). These images show that PBS and 4F treatments have little effect on airway inflammation or collagen deposition in normal C57BL/6J mice (upper images) (n = 4–6, per condition).

Immunofluorescence studies

To determine how inflammation might contribute to the mechanisms driving collagen deposition in the lungs of OVA-Sen mice, we examined sections of lungs for changes in the activation of TGFβ-1, expression of FSP-1, as well as for the presence of T15-type auto-antibodies against ox-PC and 4-HNE adducts. TGFβ-1 expression and activation are commonly increased in asthma (36). FSP-1 is expressed on fibroblasts and cells that are transitioning into fibroblasts (37). Control mice typically express low levels of TGFβ-1 (**Fig. 4**, first column, top panel). In contrast, OVA-sensitization markedly increases TGFβ-1 expression (bright green, Fig. 4, first column, middle panel) compared with PBS controls (Fig. 4, first column, top panel). 4F treatments dramatically reduced TGFβ-1 expression in the lungs of the OVA-Sen mice (Fig. 4, first column, bottom panel) to almost the levels observed in control mice (Fig. 4, first column, top panel). TGFβ-1 stimulates collagen production, promotes the transition of a variety of cells into fibroblast cells, and increases FSP-1 expression on transitioning cells. Accordingly, expression patterns of FSP-1 should parallel TGFβ-1 activation. As can be seen, control mice express low levels of FSP-1 (Fig. 4, second column, top panel). OVA-sensitized mice express high levels of FSP-1 (Fig. 4, second column, middle panel) in a pattern that was similar to the expression pattern for TGFβ-1. In contrast, 4F treatments decreased FSP-1 expression in the OVA-Sen mice to essentially the same levels as in control mice.

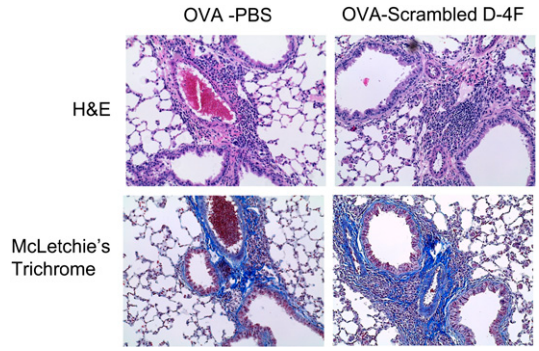

Fig. 3. Histology: effects of scrambled D-4F on pulmonary inflammation and collagen deposition in OVA-sensitized mice. Representative H and E images of sections of lungs from OVA-Sen mice treated with PBS (upper left) or scrambled D-4F (upper right). Representative trichrome images of sections of lungs from OVA-Sen mice treated with PBS (lower left) or scrambled D-4F (lower right). (n = 3, per condition).

Oxidative stress in tissue sections can be assessed immunologically using antibodies that detect well-characterized antigens, such as ox-PC and 4-HNE adducts. Control mice, which are not under chronic states of oxidative stress, typically exhibit low to nonexistent levels of T15-type auto-antibodies against ox-PC (Fig. 3, third column, top panel). In contrast, marked increases in T15-type auto-antibodies against ox-PC were observed in the lungs of the OVA-Sen mice (bright green, Fig. 4, third column, middle panel). 4F treatments reduced the levels of T15-type auto-antibodies in the lungs of the OVA-Sen mice (Fig. 4, third column, lower panel). Although fluorescent intensity for 4-HNE Michael's adducts in the lungs of OVA-sensitized mice was weak, image analysis revealed OVA-sensitization induced a modest increase in 4-HNE Michael's adduct formation, which was also reduced by 4F treatments. In contrast, fluorescent intensities staining for TGFβ-1, FSP-1, or T15-type autoantibodies were robust in OVA-Sen mice and dramatically decreased in OVA-Sen mice treated with 4F (Fig. 4, last column, bottom panel) to essentially control levels (Fig. 4, last column, middle panel). (Negative controls for the immunofluorescence studies are provided as online supplemental data.)

EPO activity and peripheral eosinophil counts

OVA-sensitization increased BALF EPO activity more than 4-fold compared with controls (**Fig. 5A**). In contrast, 4F treatments reduced BALF EPO activity in OVA-Sen mice by nearly half of that observed in untreated OVA-Sen mice (Fig. 5A). These changes paralleled peripheral blood eosinophil counts. OVA-sensitization increased peripheral eosinophil counts whereas 4F treatments decreased eosinophil counts in the OVA-Sen mice (Fig. 5B).

Total serum IgE

OVA-sensitization significantly increased total IgE levels in the mice compared with Non-Sen controls (**Fig. 6**). 4F treatments decreased IgE levels in the OVA-sensitized mice compared with IgE levels in untreated OVA-sensitized mice (Fig. 6).

Total cholesterol, HDL cholesterol, and p-HDL

OVA-sensitization and 4F treatment had no effect on total cholesterol or HDL cholesterol compared with Non-Sen

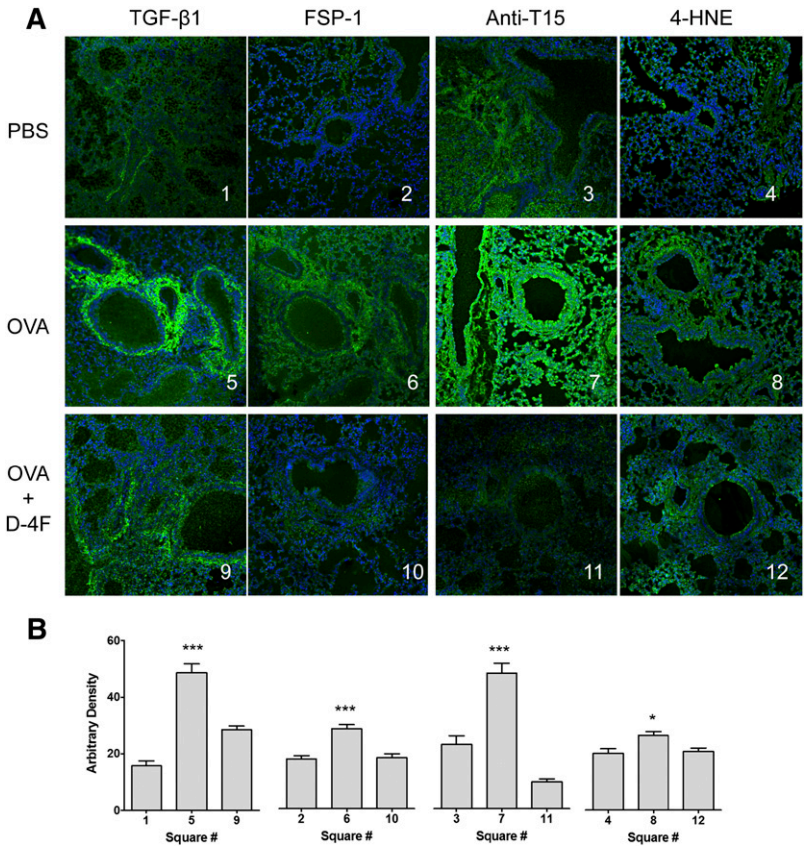

Fig. 4. Immunofluorescence studies: effects of OVA sensitization and D-4F on TGFβ-1 activation, FSP-1 expression, T15 autoantibodies, and 4-HNE Michael's adducts in the lung. Representative immunofluorescence images for TGFβ-1, FSP-1, anti-T15-type autoantibodies against ox-PC (POVPC) and 4-HNE adducts in lungs of controls (PBS), OVA-sensitized (OVA) mice, and OVA-sensitized-D-4F-treated (OVA+4F) mice (n = 4–6, per condition). Intensity of green fluorescence was quantified using NIH ImageJ software. Data are expressed in arbitrary units and presented as arbitrary density.

controls (**Fig. 7A** and B, respectively). In contrast, p-HDL was increased in the OVA-Sen mice compared with Non-Sen mice (Fig. 7). 4F treatments significantly decreased p-HDL in OVA-Sen mice compared with untreated OVA-Sen mice (Fig. 7C).

DISCUSSION

Although many recognize that HDL, and by extension apoA-I, plays an important anti-atherogenic role in coronary heart disease, logically it should also protect the vascular beds of other organs. We recently reported that apoA-I plays several important roles in protecting the lung (6). Genetic deletion of apoA-I increased AHR with respect to tissue dampening and elastance. These changes coincided with a marked increase in oxidative modification of tissue tyrosines, infiltration of inflammatory cells, and collagen deposition in the lung (6). Additional studies showed that genetic deletion of apoA-I not only increased oxidative modification of HDL but also decreased paraoxonase activity without decreasing expression (6).

In the present study, we determined the effects of 4F on airway physiology in the asthmatic mice employing the same analytical techniques used in our previous study in apoA-I knockout mice (6). Studies here showed that OVA-sensitization markedly increased airway resistance with respect to R_N, G, and H and that intranasal 4F treatments reduced AHR in OVA-Sen mice. Improvements in airway responses were most notable with respect to tissue dampening (G) and elastance (H) even though bronchoconstriction of large airways (R_N) was also reduced. Such changes in airway physiology are analogous to how 4F improved endothelium- and endothelial nitric oxide synthase (eNOS)-dependent vasodilatation in hypercholesterolemic mice, sickle cell anemia mice (16), and tight-skin mice (17). These relative changes in airway mechanics provide additional insight into the pathogenic mechanisms taking place in OVA-Sen mice treated with and without 4F.

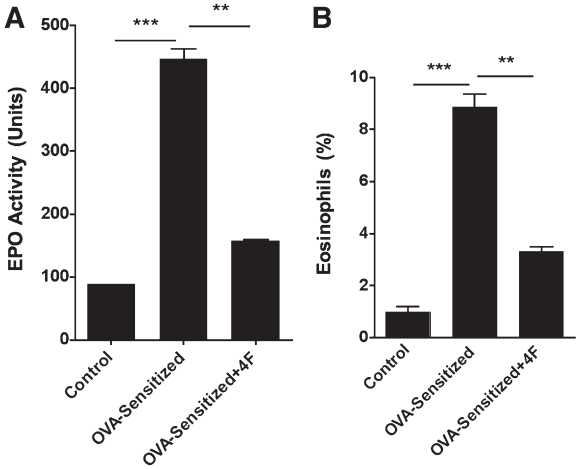

Fig. 5. Bronchial alveolar lavage fluid (BALF) EPO activity and peripheral blood eosinophil counts. A: BALF isolated from OVA-sensitized mice has higher EPO activity than controls and OVA-sensitized-D-4F-treated mice (n = 4–6, per condition). B: Similar data were observed for % eosinophils calculated from manual cell counts in peripheral blood smears (n = 4–6, per condition).

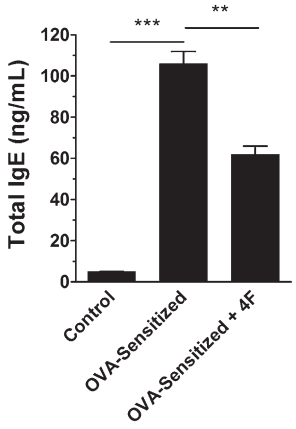

Fig. 6. Total IgE. ELISA measurements of total plasma IgE reveals that IgE levels were increased in OVA-sensitized mice (n = 11) compared with controls (n = 4) and OVA-sensitized-D-4F-treated mice (n = 4).

For example, increased collagen deposition in the perialveolar and perivascular regions of the lung is well recognized for creating stiffer lungs, which increases airway resistance with respect to tissue dampening and elastance. Trichrome staining confirms that OVA-sensitization and chronic exposure to aerosolized OVA not only increases collagen deposition in the lung but also that intranasal 4F treatments decrease collagen deposition in OVA-Sen mice.

To examine potential mechanisms driving collagen deposition in OVA-Sen mice, sections of lung were immunostained for TGFβ-1, FSP-1, anti-T15 autoantibodies, and 4-HNE adducts. TGFβ-1 stimulates collagen production as well as epithelial and endothelial mesenchymal transition into fibroblasts (38, 39). FSP-1 is a well-recognized biomarker for fibroblasts and cells that are transitioning into fibroblasts (40). AB1-2 has an absolute requirement for the canonical V_H and V_L regions of T15-type antibodies, such as EO6 (32), which have been shown to bind POVPC among various other ox-PC phospholipids (41). 4-HNE, a highly reactive breakdown product of lipid peroxidation, reacts with thiols, histidines, and lysines. When 4-HNE reacts with the free amine of lysine, it forms a covalent heterocyclic ring that is easily detected using standard immunofluorescence techniques (42). Although immunostaining for anti-T15 type antibodies and 4-HNE adducts may be an indirect means of quantifying oxidized phospholipids or 4-HNE in tissues, relative changes and patterns of staining provide important insight into which tissues and cells are experiencing marked increases in oxidative stress.

For example, in OVA-Sen mice, intense TGFβ-1 activation can be seen in the perialveolar and perivascular regions immediately adjacent to the airways and blood vessels but not immediately below or on epithelial and endothelial cells. Although the expression of FSP-1 is greatest in these same regions, it is also moderately increased throughout the parenchyma. In contrast to the pattern of TGFβ-1 activation, FSP-1 is expressed on epithelial cells and endothelial cells. This pattern of FSP-1 expression suggests that the mechanisms driving mesenchymal transition and collagen deposition extend beyond the actual site of TGFβ-1 activation. In contrast to patterns for TGFβ-1 and FSP-1, OVA-sensitization dramatically increased anti-T15 antibodies throughout the lung. Nearly every structure and cell type is positive for anti-T15 antibodies demonstrating that OVA-sensitization induced a dramatic increase in oxidative stress throughout the lung. Control immunofluoresence studies indicate that this marked increase in anti-T15 antibody staining is not a result of nonspecific IgG accumulation in the lung. Immunofluorescent staining for 4-HNE adducts shows that the increase in 4-HNE adducts in OVA-Sen mice occurs not only throughout the parenchyma but also on the surface of the epithelium and endothelium and in some regions, in a punctate

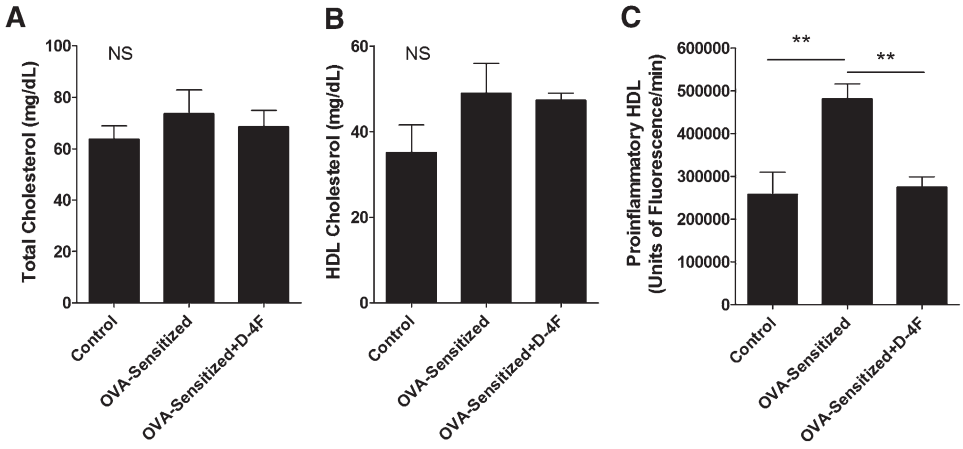

Fig. 7. Total cholesterol, HDL cholesterol, and proinflammatory HDL. A: This bar graph shows the concentration of total cholesterol in control, OVA-Sen, and OVA-Sen+D-4F-treated mice (NS = not significant). B: This bar graph shows HDL cholesterol concentrations in control, OVA-Sen, and OVA-Sen+D-4F-treated mice. C: Proinflammatory HDL (p-HDL) is a cell-free assay that assesses the oxidizability of HDL. This bar graph shows that HDL in OVA-sensitized mice is more easily oxidized than HDL isolated from control mice and that intranasal D-4F treatments decrease HDL oxidizability in OVA-sensitized mice. (NS, not significant; Controls, n = 4; OVA-sensitized, n = 11; OVA-sensitized+D-4F, n = 4).

pattern. This makes sense when one considers the fact that lipid peroxidation increases production of 4-HNE and that during inflammation hot spots of oxidation are fully capable of increasing 4-HNE to very high local concentrations (43). In this context, it is important to note that 4F treatments not only reduced the intensity of immunostaining for each analyte but also ablated these distinct patterns of activation, expression, innate immune reaction, and/or adduct formation. These data are consistent with the notion that allergen-induced experimental asthma increases oxidative stress and activates TGFβ-1, which promotes transition of epithelial and endothelial cells into myofibroblasts, which in turn increases collagen deposition. At the very least, our observations show that 4F decreases oxidative stress and TGFβ-1 activation in OVA-Sen mice and by extension that this increase in oxidative stress activates TGFβ-1 by an as yet undefined mechanism. Additional studies are required to determine how OVA-sensitization increases oxidative stress and how an increase in oxidative stress activates TGFβ-1. More importantly, additional studies are required to determine the exact mechanisms by which 4F disrupts this process to inhibit collagen deposition in the asthmatic lung.

An increase in total IgE is indicative of active allergen-induced asthma (44). IgE is expressed by B-cells under the direction of T_H2 cells in subjects with atopy (45). In subjects who do not have atopy, the relationship between total IgE and asthma is less clear. Regardless, IgE is believed to accelerate asthma by binding to mast cells and basophils which, in turn, degranulate, release histamine, and generate cytokines that exacerbate pulmonary inflammation. In this context, it is important to note that 4F significantly decreased total IgE in the OVA-Sen mice. These data provide further support for the idea that targeting oxidative stress is an important therapeutic avenue for limiting inflammation in asthma.

Our plasma lipid data confirm that asthma does not alter total plasma cholesterol or HDL concentrations but significantly increases p-HDL. These original observations support our hypothesis that asthma increases oxidative stress such that it markedly increases the oxidizability of HDL. Under these conditions, the ability of HDL to perform its normal anti-inflammatory and protective functions is likely impaired.

The exact mechanisms by which 4F inhibits experimental asthma remain unknown. What we showed here was that 4F reduces oxidative stress in the lungs and plasma of the OVA-Sen mice. 4F may reduce oxidative stress in the asthmatic lung by binding oxidized lipids, remodeling HDL, and improving HDL function. A recent report provides strong biophysical evidence that 4F has a much higher affinity for oxidized lipids and phospholipids than native lipids (46). Preferentially removing oxidized lipids from HDL should protect HDL from oxidative modification as well as HDL-associated paraoxonase from inactivation (13, 47). Thus, anything that reduces the potential for oxidation or protects paraoxonase activity would be anticipated to improve any of HDL's many functions: increasing reverse cholesterol transport (48), binding and removal of oxidative enzymes from inflamed tissues (19), stimulating pulmonary •NO production (6), inhibiting vascular $O_2^{\bullet-}$ generation (49) and inhibiting LDL-induced increases in monocyte/leukocyte chemotactic activity (9, 50).

Another way 4F may reduce oxidative stress in experimental asthma is by binding to and stabilizing ABCA1 (51). Stabilization of ABCA1 not only facilitates the transfer of native cholesterol and phospholipid but also their oxidized counterparts, which logically should also help protect the lung (52). Alternatively, 4F stabilization of ABCA1 may also activate the JAK2/STAT3 anti-inflammatory pathway to inhibit cytokine expression as was recently shown for apoA-I (53) but not for 4F (51, 53). Recent reports indicate that transgenic overexpression of eNOS reduced many of the hallmark features of OVA-induced asthma in mice (54). Earlier, we showed that 4F restored •NO and $O_2^{\bullet-}$ balance in LDL-treated endothelial cell cultures by increasing heat shock protein 90 association with eNOS (55), a protein-protein interaction that is well recognized for enhancing •NO production and decreasing $O_2^{\bullet-}$ generation from eNOS (56–58). Further, we showed that 22-hydroxycholesterol dramatically impaired •NO production and increased $O_2^{\bullet-}$ generation, collagen synthesis, and ABCA1 expression in endothelial cell cultures (19). Interestingly, adding 4F to these cultures also restored •NO production, decreased $O_2^{\bullet-}$ generation, and inhibited collagen synthesis but not ABCA1 expression, which remained increased (19). Thus, 4F may decrease inflammation in the asthmatic lung by restoring •NO and $O_2^{\bullet-}$ balance via recoupling eNOS. Accordingly, any therapy targeting eNOS-dependent •NO production may attenuate oxidative stress, inflammation, and even collagen deposition in experimental asthma.

Previously, we showed that 4F improved vasodilatation but could not reduce vessel wall thickness or decrease p-HDL in $Ldlr^{-/-}/apoA\text{-}I^{-/-}$ mice fed a Western diet (19). As 4F is fully capable of reducing vessel wall thickness in cholesterol-fed $Ldlr^{-/-}$ mice, which express apoA-I, we reasoned that the absence of apoA-I prevented or at least limited 4F from inhibiting the mechanisms by which hypercholesterolemia impairs vasodilatation and increases vessel wall thickness in these mice. With respect to experimental asthma, our recent report showing that genetic loss of apoA-I also increases pulmonary inflammation, collagen deposition, and AHR in Non-Sen mice suggests that apoA-I is important for preventing pulmonary inflammation and that 4F may inhibit experimental asthma by an HDL-dependent mechanism.

In conclusion, experimental asthma increases oxidative stress, pulmonary inflammation, and AHR in mice by mechanisms that can be attenuated by 4F, an apoA-I mimetic. Oxidative stress likely plays a central role in the mechanisms by which experimental asthma increases inflammation. Intranasal 4F reduces at least two well-established biomarkers of oxidative stress, decreases recruitment of inflammatory cells, and prevents collagen deposition, which reduces pulmonary stiffness and decreases AHR in experimental asthma. In contrast, scrambled 4F has no effect on recruitment of inflammatory cells or collagen de-

position in OVA-Sen mice. Thus, the mechanisms by which 4F reduces pulmonary inflammation and collagen deposition in experimental asthma is intimately linked to 4F's unique amphipathic structure rather than composition. Additional studies are required to determine the exact mechanisms by which 4F reduces pulmonary inflammation and AHR in experimental asthma.

REFERENCES

1. Update 2002: Expert Panel Report. NAEPP Expert Panel Report: Guidelines for the Diagnosis and Management of Asthma—Update on Selected Topics 2002. National Asthma Education and Prevention Program. (Accessed December 10, 2010, at http://www.nhlbi.nih.gov/guidelines/asthma/index.htm.)
2. Weiss, K. B., and S. D. Sullivan. 2001. The health economics of asthma and rhinitis. I. Assessing the economic impact. *J. Allergy Clin. Immunol.* **107:** 3–8.
3. Taube, C., N. Miyahara, V. Ott, B. Swanson, K. Takeda, J. Loader, L. D. Shultz, A. M. Tager, A. D. Luster, A. Dakhama, et al. 2006. The leukotriene B4 receptor (BLT1) is required for effector CD8+ T cell-mediated, mast cell-dependent airway hyperresponsiveness. *J. Immunol.* **176:** 3157–3164.
4. Bates, S. R., J. Q. Tao, H. L. Collins, O. L. Francone, and G. H. Rothblat. 2005. Pulmonary abnormalities due to ABCA1 deficiency in mice. *Am. J. Physiol. Lung Cell. Mol. Physiol.* **289:** L980–L989.
5. Otera, H., T. Ishida, T. Nishiuma, K. Kobayashi, Y. Kotani, T. Yasuda, R. K. Kundu, T. Quertermous, K. Hirata, and Y. Nishimura. 2009. Targeted inactivation of endothelial lipase attenuates lung allergic inflammation through raising plasma HDL level and inhibiting eosinophil infiltration. *Am. J. Physiol. Lung Cell. Mol. Physiol.* **296:** L594–L602.
6. Wang, W., H. Xu, Y. Shi, S. Nandedkar, H. Zhang, H. Gao, T. Feroah, D. Weihrauch, M. L. Schulte, D. W. Jones, et al. 2010. Genetic deletion of apolipoprotein A-I increases airway hyperresponsiveness, inflammation, and collagen deposition in the lung. *J. Lipid Res.* **51:** 2560–2570.
7. Bowler, R. P., and J. D. Crapo. 2002. Oxidative stress in allergic respiratory diseases. *J. Allergy Clin. Immunol.* **110:** 349–356.
8. Riedl, M. A., and A. E. Nel. 2008. Importance of oxidative stress in the pathogenesis and treatment of asthma. *Curr. Opin. Allergy Clin. Immunol.* **8:** 49–56.
9. Sedgwick, J. B., Y. S. Hwang, H. A. Gerbyshak, H. Kita, and W. W. Busse. 2003. Oxidized low-density lipoprotein activates migration and degranulation of human granulocytes. *Am. J. Respir. Cell Mol. Biol.* **29:** 702–709.
10. Ekmekci, O. B., O. Donma, H. Ekmekci, N. Yildirim, O. Uysal, E. Sardogan, H. Demirel, and T. Demir. 2006. Plasma paraoxonase activities, lipoprotein oxidation, and trace element interaction in asthmatic patients. *Biol. Trace Elem. Res.* **111:** 41–52.
11. Fitzpatrick, A. M., W. G. Teague, F. Holguin, M. Yeh, and L. A. Brown. 2009. Airway glutathione homeostasis is altered in children with severe asthma: evidence for oxidant stress. *J. Allergy Clin. Immunol.* **123**: 146–152 e8.
12. Van Lenten, B. J., S. Y. Hama, F. C. de Beer, D. M. Stafforini, T. M. McIntyre, S. M. Prescott, B. N. La Du, A. M. Fogelman, and M. Navab. 1995. Anti-inflammatory HDL becomes pro-inflammatory during the acute phase response. Loss of protective effect of HDL against LDL oxidation in aortic wall cell cocultures. *J. Clin. Invest.* **96:** 2758–2767.
13. Van Lenten, B. J., A. C. Wagner, D. P. Nayak, S. Hama, M. Navab, and A. M. Fogelman. 2001. High-density lipoprotein loses its anti-inflammatory properties during acute influenza A infection. *Circulation.* **103:** 2283–2288.
14. Navab, M., G. M. Anantharamaiah, S. T. Reddy, B. J. Van Lenten, G. Hough, A. Wagner, K. Nakamura, D. W. Garber, G. Datta, J. P. Segrest, et al. 2003. Human apolipoprotein AI mimetic peptides for the treatment of atherosclerosis. *Curr. Opin. Investig. Drugs.* **4:** 1100–1104.
15. Van Lenten, B. J., A. C. Wagner, M. Navab, G. M. Anantharamaiah, E. K. Hui, D. P. Nayak, and A. M. Fogelman. 2004. D-4F, an apolipoprotein A-I mimetic peptide, inhibits the inflammatory response induced by influenza A infection of human type II pneumocytes. *Circulation.* **110:** 3252–3258.
16. Ou, J., Z. Ou, D. W. Jones, S. Holzhauer, O. A. Hatoum, A. W. Ackerman, D. W. Weihrauch, D. D. Gutterman, K. Guice, K. T. Oldham, et al. 2003. L-4F, an apolipoprotein A-1 mimetic, dramatically improves vasodilation in hypercholesterolemia and sickle cell disease. *Circulation.* **107:** 2337–2341.
17. Weihrauch, D., H. Xu, Y. Shi, J. Wang, J. Brien, D. W. Jones, S. Kaul, R. A. Komorowski, M. E. Csuka, K. T. Oldham, et al. 2007. Effects of D-4F on vasodilation, oxidative stress, angiostatin, myocardial inflammation and angiogenic potential in tight-skin mice. *Am. J. Physiol. Heart Circ. Physiol.* **293:** H1432–H1441.
18. Nandedkar, S. D., T. R. Feroah, W. Hutchins, D. Weihrauch, K. S. Konduri, J. Wang, R. C. Strunk, M. R. DeBaun, C. A. Hillery, and K. A. Pritchard. 2008. Histopathology of experimentally induced asthma in a murine model of sickle cell disease. *Blood.* **112:** 2529–2538.
19. Ou, J., J. Wang, H. Xu, Z. Ou, M. G. Sorci-Thomas, D. W. Jones, P. Signorino, J. C. Densmore, S. Kaul, K. T. Oldham, et al. 2005. Effects of D-4F on vasodilation and vessel wall thickness in hypercholesterolemic LDL receptor-null and LDL receptor/apolipoprotein A-I double-knockout mice on Western diet. *Circ. Res.* **97:** 1190–1197.
20. Navab, M., G. M. Anantharamaiah, S. Hama, D. W. Garber, M. Chaddha, G. Hough, R. Lallone, and A. M. Fogelman. 2002. Oral administration of an Apo A-I mimetic peptide synthesized from D-amino acids dramatically reduces atherosclerosis in mice independent of plasma cholesterol. *Circulation.* **105:** 290–292.
21. Nandedkar, S. D., T. R. Feroah, W. Hutchins, D. Weihrauch, K. S. Konduri, J. Wang, R. C. Strunk, M. R. DeBaun, C. A. Hillery, and K. A. Pritchard Jr. 2008. Histopathology of experimentally-induced asthma in a murine model of sickle cell disease. *Blood.* **112:** 2529–2538.
22. Gomes, R. F., and J. H. Bates. 2002. Geometric determinants of airway resistance in two isomorphic rodent species. *Respir. Physiol. Neurobiol.* **130:** 317–325.
23. Hirai, T., and J. H. Bates. 2001. Effects of deep inspiration on bronchoconstriction in the rat. *Respir. Physiol.* **127:** 201–215.
24. Hirai, T., K. A. McKeown, R. F. Gomes, and J. H. Bates. 1999. Effects of lung volume on lung and chest wall mechanics in rats. *J. Appl. Physiol.* **86:** 16–21.
25. Schuessler, T. F., S. B. Gottfried, and J. H. Bates. 1997. A model of the spontaneously breathing patient: applications to intrinsic PEEP and work of breathing. *J. Appl. Physiol.* **82:** 1694–1703.
26. Tomioka, S., J. H. Bates, and C. G. Irvin. 2002. Airway and tissue mechanics in a murine model of asthma: alveolar capsule vs. forced oscillations. *J. Appl. Physiol.* **93:** 263–270.
27. Finotto, S., M. F. Neurath, J. N. Glickman, S. Qin, H. A. Lehr, F. H. Green, K. Ackerman, K. Haley, P. R. Galle, S. J. Szabo, et al. 2002. Development of spontaneous airway changes consistent with human asthma in mice lacking T-bet. *Science.* **295:** 336–338.
28. Schuessler, T. F., and J. H. Bates. 1995. A computer-controlled research ventilator for small animals: design and evaluation. *IEEE Trans. Biomed. Eng.* **42:** 860–866.
29. Gomes, R. F., X. Shen, R. Ramchandani, R. S. Tepper, and J. H. Bates. 2000. Comparative respiratory system mechanics in rodents. *J. Appl. Physiol.* **89:** 908–916.
30. Shaw, P. X., S. Horkko, M. K. Chang, L. K. Curtiss, W. Palinski, G. J. Silverman, and J. L. Witztum. 2000. Natural antibodies with the T15 idiotype may act in atherosclerosis, apoptotic clearance, and protective immunity. *J. Clin. Invest.* **105:** 1731–1740.
31. Bole, D. G., L. M. Hendershot, and J. F. Kearney. 1986. Posttranslational association of immunoglobulin heavy chain binding protein with nascent heavy chains in nonsecreting and secreting hybridomas. *J. Cell Biol.* **102:** 1558–1566.
32. Kearney, J. F., R. Barletta, Z. S. Quan, and J. Quintans. 1981. Monoclonal vs. heterogeneous anti-H-8 antibodies in the analysis of the anti-phosphorylcholine response in BALB/c mice. *Eur. J. Immunol.* **11:** 877–883.
33. Stepp, D. W., J. Ou, A. W. Ackerman, S. Welak, D. Klick, and K. A. Pritchard, Jr. 2002. Native LDL and minimally oxidized LDL differentially regulate superoxide anion in vascular endothelium in situ. *Am. J. Physiol. Heart Circ. Physiol.* **283:** H750–H759.
34. Navab, M., S. Y. Hama, G. P. Hough, G. Subbanagounder, S. T. Reddy, and A. M. Fogelman. 2001. A cell-free assay for detecting HDL that is dysfunctional in preventing the formation of or inactivating oxidized phospholipids. *J. Lipid Res.* **42:** 1308–1317.
35. Datta, G., R. F. Epand, R. M. Epand, M. Chaddha, M. A. Kirksey, D. W. Garber, S. Lund-Katz, M. C. Phillips, S. Hama, M. Navab,

et al. 2004. Aromatic residue position on the nonpolar face of class A amphipathic helical peptides determines biological activity. *J. Biol. Chem.* **279:** 26509–26527.
36. Williams, T. J. 2004. The eosinophil enigma. *J. Clin. Invest.* **113:** 507–509.
37. Arciniegas, E., M. G. Frid, I. S. Douglas, and K. R. Stenmark. 2007. Perspectives on endothelial-to-mesenchymal transition: potential contribution to vascular remodeling in chronic pulmonary hypertension. *Am. J. Physiol. Lung Cell. Mol. Physiol.* **293:** L1–L8.
38. Binder, C. J., K. Hartvigsen, M. K. Chang, M. Miller, D. Broide, W. Palinski, L. K. Curtiss, M. Corr, and J. L. Witztum. 2004. IL-5 links adaptive and natural immunity specific for epitopes of oxidized LDL and protects from atherosclerosis. *J. Clin. Invest.* **114:** 427–437.
39. Willis, B. C., J. M. Liebler, K. Luby-Phelps, A. G. Nicholson, E. D. Crandall, R. M. du Bois, and Z. Borok. 2005. Induction of epithelial-mesenchymal transition in alveolar epithelial cells by transforming growth factor-beta1: potential role in idiopathic pulmonary fibrosis. *Am. J. Pathol.* **166:** 1321–1332.
40. O'Riordan, E., N. Mendelev, S. Patschan, D. Patschan, J. Eskander, L. Cohen-Gould, P. Chander, and M. S. Goligorsky. 2007. Chronic NOS inhibition actuates endothelial-mesenchymal transformation. *Am. J. Physiol. Heart Circ. Physiol.* **292:** H285–H294.
41. Kobayashi, M., H. Sugiyama, D. H. Wang, N. Toda, Y. Maeshima, Y. Yamasaki, N. Masuoka, M. Yamada, S. Kira, and H. Makino. 2005. Catalase deficiency renders remnant kidneys more susceptible to oxidant tissue injury and renal fibrosis in mice. *Kidney Int.* **68:** 1018–1031.
42. Uchida, K., L. I. Szweda, H. Z. Chae, and E. R. Stadtman. 1993. Immunochemical detection of 4-hydroxynonenal protein adducts in oxidized hepatocytes. *Proc. Natl. Acad. Sci. USA.* **90:** 8742–8746.
43. Strohmaier, H., H. Hinghofer-Szalkay, and R. J. Schaur. 1995. Detection of 4-hydroxynonenal (HNE) as a physiological component in human plasma. *J. Lipid Mediat. Cell Signal.* **11:** 51–61.
44. Sunyer, J., J. M. Anto, J. Castellsague, J. B. Soriano, and J. Roca. 1996. Total serum IgE is associated with asthma independently of specific IgE levels. The Spanish Group of the European Study of Asthma. *Eur. Respir. J.* **9:** 1880–1884.
45. Mosmann, T. R., and R. L. Coffman. 1989. TH1 and TH2 cells: different patterns of lymphokine secretion lead to different functional properties. *Annu. Rev. Immunol.* **7:** 145–173.
46. Van Lenten, B. J., A. C. Wagner, C. L. Jung, P. Ruchala, A. J. Waring, R. I. Lehrer, A. D. Watson, S. Hama, M. Navab, G. M. Anantharamaiah, et al. 2008. Anti-inflammatory apoA-I-mimetic peptides bind oxidized lipids with much higher affinity than human apoA-I. *J. Lipid Res.* **49:** 2302–2311.
47. Navab, M., G. M. Anantharamaiah, S. T. Reddy, S. Hama, G. Hough, V. R. Grijalva, N. Yu, B. J. Ansell, G. Datta, D. W. Garber, et al. 2005. Apolipoprotein A-I mimetic peptides. *Arterioscler. Thromb. Vasc. Biol.* **25:** 1325–1331.
48. Tall, A. R., X. Jiang, Y. Luo, and D. Silver. 2000. 1999 George Lyman Duff memorial lecture: lipid transfer proteins, HDL metabolism, and atherogenesis. *Arterioscler. Thromb. Vasc. Biol.* **20:** 1185–1188.
49. Kruger, A. L., S. Peterson, S. Turkseven, P. M. Kaminski, F. F. Zhang, S. Quan, M. S. Wolin, and N. G. Abraham. 2005. D-4F induces heme oxygenase-1 and extracellular superoxide dismutase, decreases endothelial cell sloughing, and improves vascular reactivity in rat model of diabetes. *Circulation.* **111:** 3126–3134.
50. Gharavi, N. M., P. S. Gargalovic, I. Chang, J. A. Araujo, M. J. Clark, W. L. Szeto, A. D. Watson, A. J. Lusis, and J. A. Berliner. 2007. High-density lipoprotein modulates oxidized phospholipid signaling in human endothelial cells from proinflammatory to anti-inflammatory. *Arterioscler. Thromb. Vasc. Biol.* **27:** 1346–1353.
51. Tang, C., A. M. Vaughan, G. M. Anantharamaiah, and J. F. Oram. 2006. Janus kinase 2 modulates the lipid-removing but not protein-stabilizing interactions of amphipathic helices with ABCA1. *J. Lipid Res.* **47:** 107–114.
52. Reddy, S. T., S. Hama, C. Ng, V. Grijalva, M. Navab, and A. M. Fogelman. 2002. ATP-binding cassette transporter 1 participates in LDL oxidation by artery wall cells. *Arterioscler. Thromb. Vasc. Biol.* **22:** 1877–1883.
53. Tang, C., Y. Liu, P. S. Kessler, A. M. Vaughan, and J. F. Oram. 2009. The macrophage cholesterol exporter ABCA1 functions as an anti-inflammatory receptor. *J. Biol. Chem.* **284:** 32336–32343.
54. Ten Broeke, R., R. De Crom, R. Van Haperen, V. Verweij, T. Leusink-Muis, I. Van Ark, F. De Clerck, F. P. Nijkamp, and G. Folkerts. 2006. Overexpression of endothelial nitric oxide synthase suppresses features of allergic asthma in mice. *Respir. Res.* **7:** 58.
55. Ou, Z., J. Ou, A. W. Ackerman, K. T. Oldham, and K. A. Pritchard, Jr. 2003. L-4F, an apolipoprotein A-1 mimetic, restores nitric oxide and superoxide anion balance in low-density lipoprotein-treated endothelial cells. *Circulation.* **107:** 1520–1524.
56. Pritchard, K. A., Jr., A. W. Ackerman, E. R. Gross, D. W. Stepp, Y. Shi, J. T. Fontana, J. E. Baker, and W. C. Sessa. 2001. Heat shock protein 90 mediates the balance of nitric oxide and superoxide anion from endothelial nitric-oxide synthase. *J. Biol. Chem.* **276:** 17621–17624.
57. Pritchard, K. A., A. W. Ackerman, J. Ou, M. Curtis, D. M. Smalley, J. T. Fontana, M. B. Stemerman, and W. C. Sessa. 2002. Native low-density lipoprotein induces endothelial nitric oxide synthase dysfunction: role of heat shock protein 90 and caveolin-1. *Free Radic. Biol. Med.* **33:** 52–62.
58. Ou, J., Z. Ou, A. W. Ackerman, K. T. Oldham, and K. A. Pritchard, Jr. 2003. Inhibition of heat shock protein 90 (hsp90) in proliferating endothelial cells uncouples endothelial nitric oxide synthase activity. *Free Radic. Biol. Med.* **34:** 269–276.